CHAPTER – 1

Introduction
and
Literature Review

CHAPTER 1

INTRODUCTION AND LITERATURE REVIEW

1.1 Historical Preview

The importance of materials design and development at various timeline has predominantly influenced the human civilizations. The anthropologist often designate human life era with the materials in importance i.e. Stone Age, Bronze Age, Iron Age, Steel Age etc. [1]. The concept of alloying was witnessed in ancient times (3000 BC) with accidental discovery of arsenical bronze. This led to the development of bronze by intentional alloying of copper and tin (in 2500 BC) marking the beginning of Bronze Age. The timeline for the inception of various materials from ancient times to the modern days can be better understood with the help of Figure 1.1. From the Figure 1.1, it may be understood that the pace of materials development was not very fast due to the complexities involved in the extraction of metals from its ores. However, the industrial revolution in the year 1790 brought a paradigm shift in the development of new alloys. The alloys used for structural applications are mostly containing single metallic element (i.e. Al, Fe, Cu, Ni, Ti etc.) with the addition of other minor alloying elements to improve their properties [2]. The concept of alloys containing multi-principal elements in equitomic or near equiatomic proportion marked the beginning of era of 'High Entropy Alloys' (HEAs) [3]. Although, the word HEA was coined recently, however the concept of HEAs dates back to ancient times as evident from the existence of *panchadhatu* (an alloy of five elements) and *asthadhatu* (an alloy of eight elements) [4]. When it comes to research of equimolar alloys, Karl Franz Achard is generally regarded as the pioneer, having initially carried out his experiments in 1788 [5].

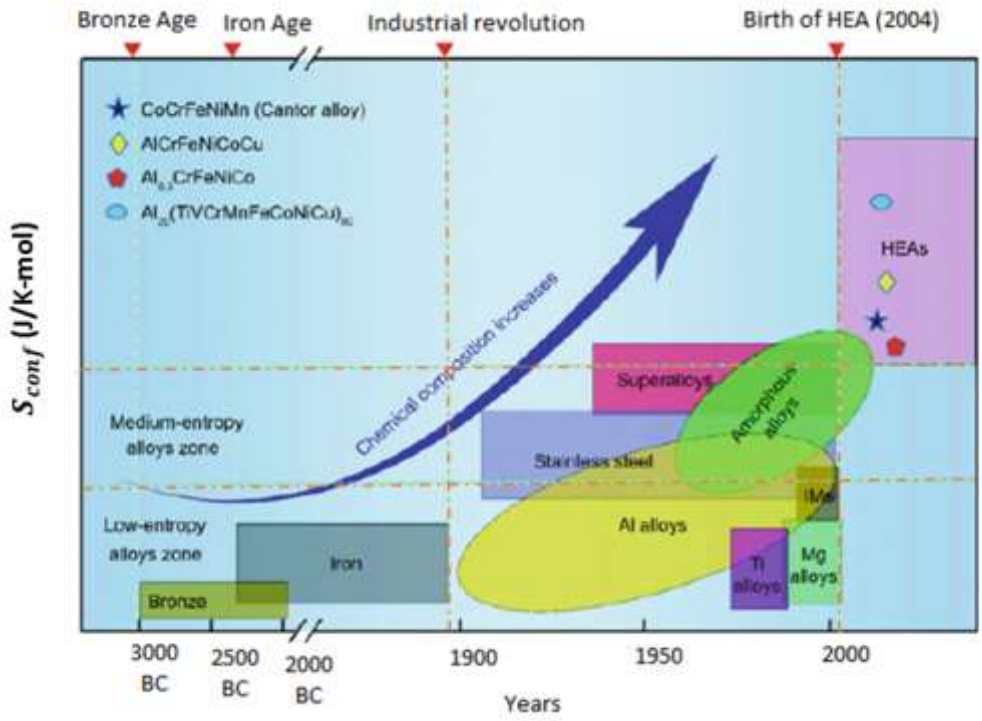

Figure 1.1: Timeline for the development of materials [2,6].

1.2 High Entropy Alloys

In 1979, Brian Cantor in U.K started working independently on multiprincipal alloys [7]. Towards the end of the twentieth century (in 1996) J. W. Yeh from Taiwan began working independently on multiprincipal alloys and named these multiprincipal alloys as 'High entropy alloys'. They were described as a High Entropy Alloys (HEAs) as an alloy comprising of at least five elements in equiatomic or near equiatomic proportion (in the range of 5 to 35 (at%) [8,9]. Based on the work so far, HEAs are considered as a potential applicants for high-temperature structural material and exhibit improved hardness, corrosion resistance, and oxidation resistance [10,11].

The high entropy alloys were classified into three major classes by Senkov and Miracle [12] and Miracle et al. [13]. There have been a total of 38 transition metals which form HEAs, like CrMnFeCoNi, which are known as transition metal based HEAs and

usually referred to as Cantor based HEAs. The second group belongs to the refractory transition metal HEAs. The main components of refractory transition metal HEAs are elements like Ti, V, Cr, Nb, Mo, Hf, Ta, and W (e.g. NbMoTaW) and commonly referred to as refractory HEAs (RHEAs). The third category is of the HEAs containing low-density elements like Li, Be, Mg, Al, Si, Sc, and Ti. These class of HEAs are usually referred to as low-density HEAs (LDHEAs).

1.2.1 Principle of High Entropy Alloys

Entropy is defined as the degree of randomness of a system. When it is considered in terms of the number of ways in which particles among themselves, a new concept of configurational entropy arises. Thus, entropy due to a particular configuration or position of constituent particles is termed configurational entropy [14]. According to Boltzmann hypothesis, configurational entropy,

$$S = k * ln(W) \tag{1.1}$$

Where W refers to the number of possible configurations and k refers to the Boltzmann constant.

$$W = \frac{n!}{n_1!n_2!n_3!.....} \tag{1.2}$$

The above equation represents the number of distinguishable ways of arrangement of n_1 number of one kind of atoms,n_2a number of other kinds of atoms and so on in 'n' different sites. The change in configurational entropy per mole ΔS_{conf} during the solid solution formation from 'n' elements with the equimolar fraction is

$$\Delta S_{conf} = R \ln(n) \tag{1.3}$$

Gibbs free energy change due to mixing is given by

$$\Delta G_{mix} = \Delta H_{mix} - T\Delta S_{mix} \tag{1.4}$$

For any process to proceed in a forward direction ΔG_{mix} should be negative for ideal solid solution as stated in equation 1.4. However, it may be pointed out that even for the case of non-ideal solutions, for solid solution formation from the pure components of the same crystal structure, $\Delta G = \Delta G_{mix}$ and thus the criteria $\Delta G < 0$ and $\Delta G_{mix} < 0$ are identical. If the crystal structures of any of the components and the solid solution are different, then one must also consider the free-energy change of the crystal structures of the components to that of the solid solution and thus the criterion $\Delta G < 0$ must be considered for such situations. Thus in general, one should use the criterion $\Delta G < 0$ rather than $\Delta G_{mix} < 0$.

Also, at constant volume or heat content, ΔS_{conf} is the major contributor to ΔS_{mix} and by equation (1.3) ΔS_{conf} increases on increasing n, number of components and reaches its maximum when the concentration of each element is equal. Hence, on increasing number of factors, each with equal concentration, ΔS_{mix} will increase enormously, making ΔG_{mix}more and more negative. The tendency to decrease free energy encourages the emergence of a single solid solution phase, compared to lower ΔS_{conf} of intermetallics. This feature forms the basis of HEAs. However, a solid solution is not always favoured. Depending on the processing route utilized, intermetallic and bulk metallic glasses have been found to form in HEAs. Hence, the role of entropy information of a single SS phase needs further investigation.

1.2.2 Configuration Entropy based Classification

J.W. Yeh gave a new classification of alloys on the basis of configurational entropy. According to this, alloys having ΔS_{conf}<R is considered to be low entropy alloys [15,16]. Those having 1.5R<ΔS_{conf}>R are considered to be medium entropy alloys, and any metallic system, whether it is intermetallic, bulk metallic glasses, or SS, is deemed to be high entropy alloy provided it has ΔS_{conf}>1.5R.

1.2.3 The Four Core Effects

The phase stability and mechanical properties of HEAs are governed by the four core effects. The four core effects influencing the properties and stability of HEAs are mentioned as follows:

a) High entropy effect

b) Lattice distortion effect

c) Sluggish diffusion effect

d) Cocktail effect

Table 1.1: Classification of various metallic systems based on ΔS_{conf} [8].

SYSTEM	ALLOYS	ΔS_{conf}
Low alloy steel	4340	0.22R low
Stainless steel	304	0.96R low
	316	1.16R medium
High Speed steel	M2	0.73R low
Mg alloy	AZ91D	0.35R low
Al alloy	2024	0.29R low
Ni-base superalloy	Inconel 718	1.31R medium
Co-base superalloy	Stellite 6	1.13R medium
BMG	$Cu_{47}Zr_{11}Ti_{34}Ni_8$	1.30R medium
HEA	ALLOYS	≥1.5R high

(a) High Entropy Effect

As per the second law of thermodynamics, the equilibrium state of an alloy is defined as the one with the least free energy of mixing. Under the alloy's lowest melting

point, three sorts of contending stages are conceivable: elemental phases, intermetallic complexes, as well as solid solution phases [17]. The most basic is a single solid solution. Intermetallic compounds, such as NiAl, have superlattices that make them distinctive, such the B2 configuration. A solid solution phase is the one where all of the constituents bearing BCC, FCC, or HCP structure are all intermixed or mixed fully. Solid solutions, although they are more randomly organized, co-exist with intermetallic compounds [18,19].

By increasing the number of components in an alloy, one can raise its configurational entropy, which favors the formation of a single-phase solid solution. Nevertheless, intermetallic formation in conjunction to solid solution is also feasible in high entropy alloys. It is obvious that, there are really additional factors that are critical in controlling various other phase formations in multi - component alloys.

(b) Severe Distortion Effect

The varied atom sizes that build up the crystal lattices of multi-component alloys cause severe lattice deformation. The occupancy at every lattice location is determined by the atom which resides there and the kinds of atoms within surroundings. These aberrations, are much more serious than those found in conventional alloys. The extreme lattice deformation phenomenon is frequently compared to alloys with a single dominating element, in which the lattice location is primarily taken by the major ingredient. For HEAs, every element gets an equal chance of occupying a lattice location. Due to the fact that the sizes of individual elements might vary significantly in certain circumstances, it can result in serious lattice deformation [20]. Yeh et al. [21] investigated the anomalous reduction in the X-ray diffraction (XRD) intensity of CuNiAlCoCrFeSi alloy systems with several primary elements.

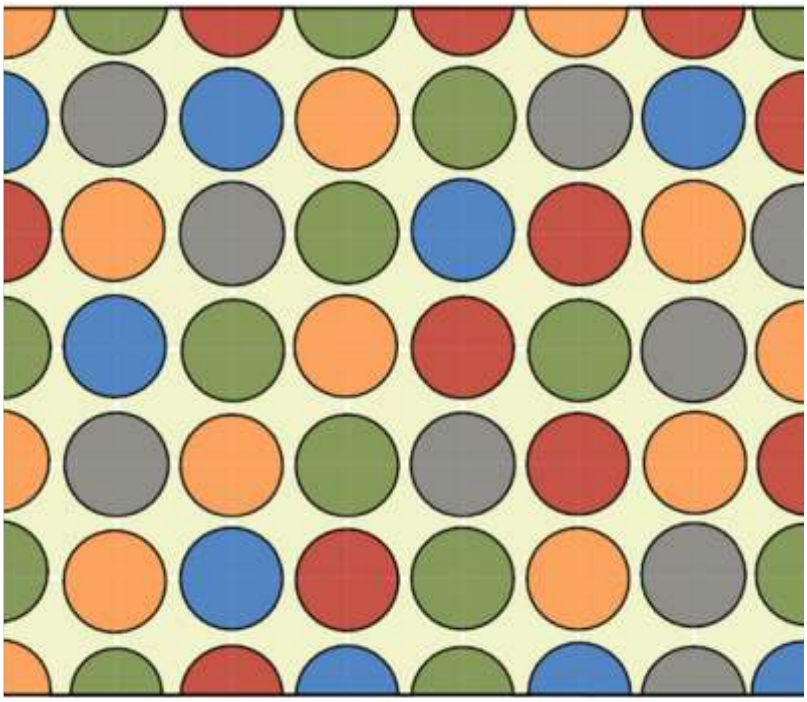

Figure 1.2: The depicted notion of random mixing of components in a multi-component alloy, as indicated by the circles in various colors. With equal atom sizes and loose atomic packing implied, the configuration entropy of mixing the alloy is identical to that of an ideal gas, and so is maximized by the use of an equiatomic composition design [22].

A sequence of CuNiAlCoCrFeSi alloys with a deliberate inclusion of major components (range from pure components to seven members) was subjected to quantified analysis of XRD intensity. The fluctuation in the alloy system's XRD peak intensities is similar to that caused by temperature influences. The significant lattice distortion also helps explain the high strength of HEAs, particularly those with a BCC structure [23–25]. The strong lattice distortion effect is likewise associated with tensile brittleness and delayed kinetics [9,26,27] in HEAs. The single-phase FCC-structured HEAs are inherently weak and cannot be attributed to the substantial lattice deformation [28].

(c) Sluggish Diffusion Effect

It has been suggested that HEAs have slower diffusion and phase change kinetics than their conventional counterparts [29]. Due to the diversity in local atomic configurations, each site has a unique bonding and local energy configuration. Whenever

an atom approaches a region with relatively low energy, it is termed to be 'trapped' and there will be a decreased chance of leaping from that location. In comparison, if indeed the location is a high energy location, the atom does have a greater probability of returning towards its originating location and such circumstances leads to a slower diffusion rate. Second, each element in a HEA has a unique diffusion rate. Certain components have a lower level of activity than the others (e.g., the ones having high melting temperatures), and thus have a lower success rate of filling voids when competing with other elements.

Table 1.2: Diffusion indices for Ni in various FCC matrices. The compositions of Fe-Cr-Ni(Si) alloy are given in wt.% [30].

Solute	System	D_o	Q	T_m	Q/T_m	D_{T_m}
Ni	CoCrFeMnNi	19.7	317.5	1607	0.1975	0.95
	FCC Fe	3	314	1812	0.1733	2.66
	Co	0.43	282.2	1768	0.1596	1.98
	Ni	1.77	285.3	1728	0.1651	4.21
	Fe-15Cr-20Ni	1.5	300	1731	0.1733	1.33
	Fe-15Cr-45Ni	1.8	293	1697	0.1727	1.73
	Fe-22Cr-45Ni	1.1	291	1688	0.1724	1.09
	Fe-15Cr-20Ni-Si	4.8	310	1705	0.1818	1.53

(c) Cocktail Effect

The traits of HEAs are inextricably linked to those of their subcomponents. For instance, the inclusion of light components reduces the alloy's density. However, in addition to the qualities of the constituent pieces, the interaction of the constituent elements should

be addressed. For instance Al is an element which is malleable and possesses low-melting-point, however its inclusion might result in the hardening of HEAs. This occurred partially due to the formation of a hard BCC phase and partially as a result of Al's stronger cohesive bonding with other elements and its bigger atomic size. Therefore, the macroscopic characteristics of HEA are obtained through the averaged characteristics of its constituent elements and take into account the impacts of surplus qualities produced by inter-elemental interaction as well as lattice deformation [31,32]. Refractory HEAs are mostly composed of refractory materials with melting points more than 1650 ℃. According to the rule of mixtures, the melting points of quaternary equiatomic alloy MoNbTaVW and quinary equiatomic alloy MoNbTaVW are more than 2600 ℃. Both alloys exhibit significantly greater ductility over superalloys and therefore have yield strengths more than 400 MPa at 1600 ℃ [33]. Thus, these HEAs are predicted to have considerable promise in those tasks involving extremely high temperatures. Zhang et al. [28] investigated $CoNiFe(AlSi)_{0.8}$ alloys in order to get the optimal mixture of electric, magnetic, and mechanical characteristics. Zhang et al. [28] investigated $CoNiFe(AlSi)_{0.8}$ alloys in order to get the optimal confluence of magnetic, electrical, and mechanical characteristics. $CoNiFe(AlSi)_{0.2}$ is indeed the finest alloy, having a saturated magnetism of 1.15 T, a coactivity of 1400 A/m. This alloy also possess an electric resistivity of 69.5 μΩ-cm, an ultimate tensile of 342 MPa, as well as strain without breakage (50%). This indicates the alloy's superiority as a soft magnetic element for a wide variety of possible purposes [28]. The whole observation has been achieved on an alloy configuration that incorporates equiatomic ferromagnetic components (Fe, Co, and Ni) to form the FCC phase (atomic packing density greater than BCC), as well as the inclusion of nonmagnetic components (Al and Si with mildly antiparallel magnetic coupling to Fe, Co, and Ni) to enhance deformation. As a

consequence, it produced a beneficial cocktail effect, resulting in increased magnetization, reduced coercivity, excellent plasticity, higher strength, and excellent voltage resistance.

1.2.4 Phase Prediction Rules in HEAs

The high entropy of mixing seems to be the dominating factor for solid-solution formation in HEAs. However, many a times multicomponent alloys with high entropy of mixing result in the formation of intermetallics or amorphous phases. Zhang et al. [23] considered two more factors other than entropy responsible for solid-solution formation. They are atomic size difference (δ), enthalpy of mixing (ΔH_{mix}) and entropy of mixing (ΔS_{mix}) decribed as follows:

(a) Atomic Size Difference (δ)

$$\delta = \sqrt{\sum_{i=1}^{n} C_i \left(1 - \frac{r_i}{\bar{r}}\right)^2} \tag{1.5}$$

Where $\bar{r}$=$\sum_{i=1}^{n} C_i\, r_i$ is average atomic radii and r_i is the atomic radii of i^{th} element, n denotes the number of constituents in an alloy system however, C_i is the i^{th}component's atomic percentage.

(b) Enthalpy of Mixing (ΔH_{mix})

$$\Delta H_{mix} = \sum_{i=1, i\neq j}^{n} \Omega_{ij}\, C_i\, C_j \tag{1.6}$$

Where Ω_{ij}(=4ΔH_{AB}^{mix}) is a regular melt-interaction parameter among i^{th} and j^{th}elements and the mixing enthalpy of binary AB alloy is ΔH_{AB}^{mix}.

(c) Entropy of Mixing (ΔS_{mix})

$$\Delta S_{mix} = -\mathrm{R}\sum_{i=1}^{n}(C_i \ln C_i) \tag{1.7}$$

The findings of Zhang et al. (2008) suggested that having atomic size discrepancies smaller than 6.5% but rather enthalpy of mixing qualities in the range of −15 to 5 kJ mol^{-1} are necessary to construct solid-solutions in multicomponent alloys; thus, solid-solutions can be formed only if the atomic size discrepancies are under 6.5% and indeed the enthalpy of mixing is between −15 and 5 kJ mol^{-1}.

Recently Yang & Zhang [34] introduced a new parameter **Ω** and defined it as

$$\Omega = \frac{T_m \Delta S_{mix}}{|\Delta H_{mix}|} \tag{1.8}$$

Here $T_m = \sum_{i=1}^{n} C_i (T_m)_i$. T_m denotes the melting point of the n-elements alloy, whereas $(T_m)_i$ denotes the melting point of the ith component of the alloy.

Their analysis is that when $\Delta H_{mix} < 0$, compound formation takes place, and when $\Delta H_{mix} > 0$, segregation or phase separation occurs. Consequently, they assumed that both the cases resist the formation of solid solution. Also $\Delta S_{mix} > 0$ favors solid solution formation. Thus, the formation of solid solutions may be judged by $T\Delta S_{mix}$ and $|H_{mix}|$. **Ω** ≥1 is favorable for solid solution formation as in this case entropy dominates over enthalpy, and when **Ω**<1 enthalpy dominates over entropy favouring intermetallics or segregation. They considered atomic size difference (δ) and suggested a relation among δ and **Ω** for multicomponent alloys. They recommended that for HE stabilized solid solution **Ω** ≥1 and δ < 6.6.

Apart from above-mentioned criteria, Guo et al. [35] found that the valence electron concentration (VEC) plays an significant role in predicting the structure of phase which may be formed. The VEC of multicomponent alloy system can be calculated as defined in the equation 1.9. The VEC for an 'N' component system can be computed [35] as:

$$VEC = \sum_{i=1}^{N} x_i (VEC)_i \tag{1.9}$$

Based on the value of the VEC computed the structure can be predicted as follows: $VEC < 6.87$ BCC phase, $VEC > 8$ FCC phase, and $6.87 \le VEC \le 8$ BCC + FCC phase.

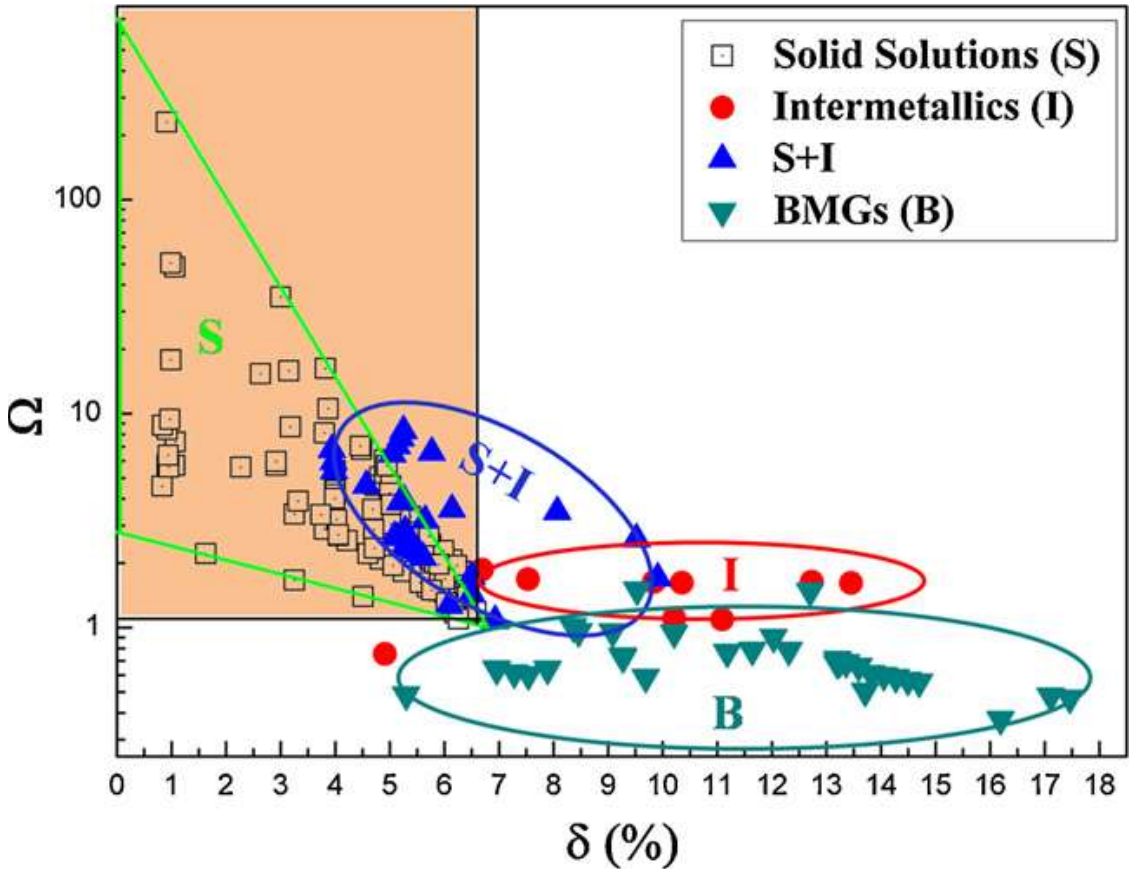

Figure 1.3: Demonstrates the relationship among the parameters δ and Ω for multi-component alloys. Here "Solid Solutions" implies that the alloy is composed entirely of solid solution; "Intermetallics" demonstrates that the alloy is composed primarily of intermetallic compounds and other ordered phases; "S+I" implies that in multi-component alloys, not only solid solution but also ordered compounds can precipitate; and "BMGs" implies that the alloy is composed entirely of amorphous phase [36].

1.3 Synthesis and Processing Routes for HEAs

Various synthesis routes have synthesized HEAs. Such routes can be divided into three main categories: route of melting/casting, route of solid-state processing, and deposition techniques. Melting/casting routes are commonly used for the synthesis of the HEAs from these three processing routes.

1.3.1 Vacuum Arc Melting (VAR)

Vacuum arc melting [37] has created a large number of HEAs. It utilizes the arc for higher temperature melting of various metals. This approach is not appropriate for melting low melting temperature (Tm < 600 ºC) metals due to their elevated vapor pressure, i.e., Mg, Zn, Mn, etc.

1.3.2 Vacuum Induction Melting (VIM)

Metals with low melting points are typically melted by vacuum induction melting (VIM). To melt the charge material, VIM uses the heat produced by the eddy current caused by electromagnetic induction. The formation of the heterogeneous microstructure [24] is the major drawback associated with the melting/casting path. The consequence of the slow rate of solidification is this heterogeneous microstructure. This will result in the formation of microstructure dendritic (DR) and inter-dendritic (ID) segregations [38]. However, in some situations, the development of inter-dendritic regions is difficult to prevent. Alternatively, at room temperature, annealing at a higher temperature and then followed by quenching will produce a single stage. A faster solidification method, i.e., suction casting, injection casting, drop-casting, splat quenching, and melt spinning, should be used to obtain the single-phase microstructure by melting/casting path [39]. Li et al. [40] conducted an earlier study on the impact of magnesium addition on the microstructure, density, and mechanical characteristics of $Mg_x(MnAlZnCu)_{100-x}$ (x= 20, 33, 43, 45.6, 50 at%) alloys. These as-cast magnesium-based HEAs produced by induction melting contain a significant HCP phase that is immersed in Al-Mn icosahedral quasicrystal precipitates with lower density (2.20–4.29 g cm^{-3}), higher hardness (1.78–4.29 GPa), as well as higher compressive strength (400–500 MPa) at room temperature [40]. These alloys, especially equiatomic MgMnAlZnCu alloys, exhibit excellent thermal stability up to 677 °C (950 K). Though they possess the lower density, high thermal stability, and strength,

these HEAs break spectacularly beneath certain load due to their lack of ductility (with a failure strain of ~ 3–5%). Sanchez et al. [41] recently reported the vacuum die-casting of $Al_{60}Cu_{10}Fe_{10}Cr_5Mn_5Ni_5Mg_5$ LDHEA.This LDHEA has a low density of 4.6 g cm^3 as well as a significant hardness of 9.16 GPa, it exhibits a dendritic microstructure composed of complicated intermetallics such as Al_3Ni_2, Al_7Cu_4Ni, and $Mg_2Cu_6Al_5$ [42]. Homogeneity in the structure as well as microstructure of the finished product is a significant issue [43,44]. Additionally, the low vapor pressure elements such as Mg, Zn complicate the melting and solidification processes. In comparison to melting/casting route of processing, the solid-state route of processing has produced a modest proportion of HEAs [45].

1.3.3 Mechanical Alloying (MA)

Mechanical alloying (MA) a top-down approach to the processing of nanocrystalline materials, is essentially included in this route [46]. Flattening, cold welding, fracturing, and re-welding powder particles trapped among the balls are all steps in the alloying procedure [47]. It could be interpreted as the high impact forces of the balls deforming the powder particles plastically, leading to hardening and fracturing of the work. The new surfaces on the broken particles allow them to weld together and shape larger sizes (due to the nature of softness). At the end of milling, the different combinations of starting materials would have a layered structure of particles. The powders would become work-hardened and fractured upon further deformation. This cycle continues until the fracture dominates the cold welding to a point. To this end, the particle sizes will remain constant, and the particle structure will be gradually optimized. A steady-state condition is reached after a certain time period among the rate of welding and the rate of fracturing. At this point, the distribution of particle sizes containing all the constituent elements will be narrower. Apparently, the strong deformation during MA is attributable to several defects, i.e. dislocations, vacancies, stacking faults, and increased grain limits. These defects

increase the diffusivity of solute atoms. In addition, the refined microstructural function decreases the distance of diffusivity. A small rise in temperature during powder milling is also supported by diffusion kinetics [47–49].

Originally, this route was built to manufacture superalloys of oxide dispersion reinforced (ODS) nickel and iron base [50]. A variety of alloy phases, i.e., solid solutions, intermetallics, ordered compounds, amorphous structures, nanocomposites, and quasicrystalline phases, were successfully applied to synthesize MA, including immiscible structures. This technique also provides the benefit of extended solid solubility. This can be attributed to increased diffusion rates due to the pre-alloying nano-size of the powder component [51]. This processing route also has the potential issue of powder contamination and the above-mentioned advantages of MA [52,53]. The proper selection of milling media and the use of the inert atmosphere during MA [45] can overcome this problem. The first group to synthesize the nanostructured HEAs [54] by MA was Murty *et al.*[55]. The formation of the single-phase BCC structure in equiatomic AlFeTiCrZnCu HEA was shown by 20 h milled powder.

For addressing the issues concerned with weight loss and element segregation throughout liquid metallurgical methods, a strong emphasis has been placed on the preparation of this LDHEA via powder metallurgical procedures. Numerous researches have contributed significantly to the contemporary development of low-density HEAs by mechanical alloying (MA) accompanied by sintering. Youssef et al. [56] demonstrated the development of a single-phase solid solution in $Al_{20}Li_{20}Mg_{20}Sc_{20}Ti_{20}$ HEA, prepared through mechanical alloying technique for 6 h. They found that the milled powder does have an FCC configuration and a hardness of 5.8 GPa due to the nanostructured granules of 12 nm. This lightweight HEA structure turns into an HCP

structure with further annealing at 500 °C (773 K). It preserves its nanocrystalline structure, nevertheless, having a granular size of 26 nm as well as a hardness of 4.9 GPa [56]. Chen et al. [57] synthesized amorphous BeCoMgTi and BeCoMgTiZn HEAs by mechanical alloying elements with an HCP crystal structure.

1.3.4 Spark Plasma Sintering (SPS)

The consolidation of milled powder is difficult and required for better bulk characteristics. Sintering plays an important role in these nanostructured materials being densified. Sintering is a method in which particle bonding takes place by atom diffusion. It can be defined as solid-state, phase of liquid and reactive sintering. Conventional sintering (less pressure) takes more time and results in significant grain growth during high-temperature exposure.

All the above issues have been resolved to some degree by Spark plasma sintering (SPS) and can be used to consolidate the nanocrystalline alloy powder [58–61]. SPS uses a high-pulsed current through the alloy powder, which is kept inside the graphite die when the pressure application is simultaneously arranged. The plasma is stimulated at the particle-particle interfaces over a short time period, resulting in the instant heating of the powder [8]. This short period of soaking time helps to maintain the nanostructured nature of alloy powder compaction. Therefore, the sintering temperature and pressure should be carefully selected, although it affects the nanocrystalline behavior of the pellet.

Kumar and co-workers recently made a major addition to our knowledge of the influence of magnesium on the microstructure of LDHEA fabricated through SPS [62–64]. Maulik and Kumar [64] tried to synthesise $Mg_xAlCrFeCu$ (x = 0, 0.5, 1.0, and 1.7 at %) LDHEAs by MA and spark plasma sintering (SPS). After 20 h of MA with AlCrFeCu and $Mg_{0.5}AlCrFeCu$ LDHEA, a two-phase configuration comprising BCC as major and FCC

as minor phase, was formed. However, two BCC phases were generated when the quantity of Mg in $Mg_xAlCrFeCu$ (x = 1.0, 1.7) LDHEA was increased. The BCC phase fraction with a lattice parameter near to Fe enhances the atomic proportion of Mg in these LDHEA. It is thermally stable up to 500 ℃ (773 K). SPS was exploited to consolidate $Mg_xAlCrFeCu$ LDHEA at 800 °C (1073 K) [64]. Maulik et al. [63] also observed the transition of two-phase LDHEA powder into a B2-AlFe (major) phase along with a $MgCu_2$, Mg_2Cu, as well as BCC phases.

1.3.5 Other Consolidation Techniques

Apart from SPS, vacuum hot pressing and sintering (VHP), hot isostatic pressing (HIP), and microwave heating may also be used to consolidate HEA powder [65–67]. Veronesi *et al.*[68] Investigated the impact of Si modifier over microstructure and hardness of HEA-based MnFeNiCu microwave. Si free HEA showed the microstructures of Fe rich dendritic and Cu rich interdendritic regions, and Si added HEA resulted in forming an acicular structure with a higher hardness value.

1.3.6 Thin Films of HEAs

There is an essential contribution in the HEA literature to the deposition route for synthesizing the HEAs. This path essentially protects the different deposition techniques involving vapor and liquid states. Two approaches have been quite popular among vapor-based surface modifications namely plasma nitriding and magnetron sputtering. Numerous investigations attempted to deposit thin films of HEA on the substrate surface of materials like as mild steels, aluminum alloys, and HEAs in order to improve resistance to corrosion, resistance to oxidation as well as wear resistance. The vapor deposition is a procedure employed for accumulating metal, non-metal, or coatings of compounds on the substrate in the gaseous phases. Evaporative coatings, sputter coatings, and ionic coatings are the three

primary types of physical vapor deposition technique. To enhance tribological properties, AlCoCrCuFeNi high entropy alloy particles are laser surface alloyed on a Ti–6Al–4V substrate [69]. Due to the strengthening of the solid solution and the creation of intermetallics, the alloyed laser specimen exhibits greater wear resistance as compared to the substrate. By laser cladding AlTiVMoNb onto a Ti-6Al-4V (TC4) substrate, a lightweight coating was formed that enhanced the low hardenability as well as oxidation at higher temperatures [70].

1.4 Important Classes of HEAs

Several HEA investigations seem to be driven by the idea that alloys phases having a higher configurational entropy favor single-phase SS phases [9,15]. The initial objective was to explore the inner regions of hyper-dimensional compositional space, far beyond vertices, edges, as well as faces, but HEA research has advanced to include the quest for single-phase solid solutions. However, not all high entropy alloys produce single phase solid solutions. Formation of intermetallics have also been reported in the literature. Thus though the entropy is an important factor responsible for phase evolution but additional factors like enthalpy (average) as well as enthalpy between binary pairs lead to the phases actually observed.

1.4.1 Solid-Solutions

Disordered phases of solid solution have a single crystal lattice and therefore do not exhibit LRO. They might or might not have SRO-related symptoms. The configurational entropy is suggested to favor the SS phase in HEAs, with the configurational entropy determined using the Boltzmann model. A phase devoid of crystal structure is referred to as nanocrystalline, amorphous, or glassy. Irrespective of its compositional range, a phase composed of two or more chemically distinct sublattices and therefore having chemical LRO is categorized as ordered, intermetallic (IM), or compound. The typical A_xB_y

nomenclature, as well as the Strukturbericht notation, a Pearson symbols or a conventional name (like Laves or sigma), as well as the prototypical compounds, are all employed to denote IM phases. The packing fraction of the atoms determines the particular kind of SS phases (FCC, BCC, and HCP). According to the literature, HEAs with BCC structures have superior mechanical qualities, i.e., greater strength, than those with FCC structures. Gao et al. [71] conducted a literature survey and presented a tabular form of a significant number of alloys together with experimental evidence confirming their single nature. Binary component formation enthalpies are essential in the development of phases in HEAs.

a. HEAs with BCC structure

The fundamental premise is that if two components have a strong propensity to merge or phase splitting, it would be challenging to create a solid solution with single-phase. Every pair of the compound's mixing enthalpies must be evaluated. To produce a single phase, it is necessary to choose alloys where no pair exhibits a significant driving force towards formation of intermetallics or separation of phases. Thus, in addition to the average mixing enthalpy, the collection of enthalpies' extreme values must be included when phase prediction in multi-component alloys is performed[72].Compared to individual components, the reality of stabilizing the single-phase BCC structure is more reliant on the binary pairing may be better understood by taking the example of AlCoCuNiTiZn HEA into account. During room temperature, neither of the component elements have the BCC structure, however the alloy produces a single-phase after processing [73]. AlCoCuNiTiZn HEA has a significant propensity for forming binary compounds with AlFe, AlNi, AlCo, and AlTi that crystallize as a result of the creation of the d-p orbital there in BCC lattice.

Wang *et al.* [74] stated that in promoting the BCC lattice, the concentration of Al plays an important role. If the content of Al is less than 11%, it enhances the FCC; instead of that, it stabilizes the BCC structure. On the other hand, individual elements consisting

of the BCC structure also promote the formation of the BCC phase. Phase type predictions in HEAs are made qualitatively, forming components similar to the H-R rules. Generalizing assumptions are not possible because they are comprehensive, simply due to the presence of multiple elements. The refractory High Entropy Alloy (RHEAs) systems, that are largely made of components like as Cr, Hf, Mo, Nb, Ta, V, W, and Zr (e.g., that produced by Senkov et al. [75–78]. Their main phase is cubic, having a body-centered cubic (BCC) configuration (or occasionally a B2 configuration).

b. HEAs with FCC structure

As noted previously, the generation of stages in HEAs is more dependent on binary constituents than on single elements. Otto et al. [72] investigated variants on the "Cantor" alloy CoCrFeMnNi by substituting an element with equal crystallinity for one of the constituents. Structure and dimensions. For instance, substituting Cu for Ni leads in a multiphase alloy, despite the fact that Ni and Cu form an excellent solid solution.

Binary components solidify in the structure of the FCC throughout the phase formation process. Wu et al. [79] examined whether all possible subdomains (ternary, quaternary and binary) for the Cantor alloy FCC CoCrFeMnNi produce solid solutions, as both by casting and as annealing. Zhang et al. [80] demonstrated the formation of a single-phase FCC structure in CoCrFeMoNi HEA via mechanical alloying and identified several single-phase FCC solid solutions, including three of the five probable quaternary systems: CoCrFeNi, CoFeMnNi, FeMnNi, CoCrNi, and CoMnNi; CoFeNi, CrFeNi, FeMnNi, CoCrNi, and CoMnNi as five of the ten prospective ternary systems, whereas FeNi and CoNi as two of the ten probable binaries.

Table 1.3: Enthalpy matrix relevant to the Al-Li-Mg-Sc-Ti alloy (in kJ/m).

	Mg	**Al**	**Sc**	**Ti**	**Li**
Mg	0	-2	-3	16	0
Al	-2	0	-38	-30	-4
Sc	2	-38	0	8	12
Ti	16	-30	8	0	34
Li	0	-4	12	34	0

c. HEAs with HCP structure

There exist relatively less reports of the single-phased HCP structures forming in HEAs. The crystallization of the HCP structure is, in most cases, followed by other steps. Li et al. [81] observed the development of the HCP phase in $Mg_x(AlCuMnZn)_{100-x}$ (x=20,33,43,45.6,50) alloy as well as existence of the quasicrystalline phase in as-cast $Mg_x(AlCuMnZn)_{100-x}$ (x=20,33,43,45.6,50 at%) alloys [82]. Miracle *et al.* [12] stated that only seven alloys, which belong to three diverse groups of alloys are namely (i) group of light metals, group of 4f transition metals, as well as additional CCAs, are also involved in the HCP process. It was discovered that there are no common elements in the family of these alloys. No single step of HEA via MA [45] has been synthesized with an HCP structure.

There are several studies available on more than two phases alongside the single-phase HEAs. Most multiphase HEAs are processed via the processing route of equilibrium. Path of non-equilibrium production, i.e., MA, due to prolonged solid solubility, is more likely to form single-phase HEAs. Numerous HEA investigations have shown that when

the atomic size variation amongst the atoms is large or when certain components exhibit a significant affinity among them, the development of simple random solid solution phases cannot be controlled only by configuration entropy. Different intermediate phases e.g., B2, $L1_2$, sigma (σ) phases, and Laves phases have been reported more frequently in the literature in such cases [7,83–85]. Yadav et al. [84] synthesized a single intermetallic Laves phase in an equiatomic TiZrVCrNi high entropy alloy by applying the conventional melting as well as melt spinning method. We observed the formation of a nanocrystalline Laves C14 type phase in as-cast and melt-spun alloys. Thorough investigations on the phase development of mechanically alloyed (MA) $AlFeCuCrMg_x$ (x=0, 0.5, 1, and 1.7 at%) have also been reported [64]. The findings show that a solid solution phase with BCC structure develops at x = 0, 0.5 HEAs while two BCC phases develop in x = 1, 1.7 HEAs. The XRD examination of sintered alloys confirmed the formation of two BCC phases in the AlFeCuCr alloy and more complex configurations in the $AlFeCuCrMg_x$ (x = 0.5, 1, 1.7 at%) alloys, which include AlFe, BCC, and Cu_2Mg phases.

In a low-density HEA (LDHEA) $Al_{20}Li_{20}Mg_{10}Sc_{20}Ti_{30}$ alloy [86], synthesized by ball milling and forms a single-phase FCC configuration that further transforms into a single-phase HCP configuration while annealing. The above mentioned system is noteworthy in many ways: first, since Al combine with Li, Sc, and Ti, to form Al-Li, Al-Sc, and Al-Ti intermetallics beyond the melting point of Al. Additionally, Li-Ti and Li-Sc have no solubility in the solid phases anywhere at temperature (although Ti has minimal dissolution in fluid Li below the boiling point of Li). The strongly favorable Al-Sc and Al-Ti involvements are similarly noticeable, as are the strong repulsion-inducing Li-Sc and Li-Ti. These can be better understood with the help of binary enthalpy of mixing as shown in the Table 1.3. But despite these strong engagements conceivable, the alloy forms single phase FCC and changes to Single phase HCP at higher temperature. Thus, the phase

formation in this alloy system cannot be explained by the binary enthalpy estimates of pairings.

1.4.2 Low-Density HEAs (LDHEAs)

The increased demand from the energy and transportation industries, lightweight HEAs (LWHEAs) have garnered interest. However, developing LWHEAs is difficult due to the scarcity of light and affordable components. Over the last few decades, the use of lightweight vehicles has increased daily in order to cut fuel consumption and vehicle emissions. Various kinds of intermetallic evolve with the addition of Li and Mg as constituent of the high entropy alloys (HEAs) [82,87]. Nowadays, the automobile industry places a premium on lightweight environmentally friendly materials (LWEFMs), such as aluminum, plastics, magnesium, and composites, due to their numerous intrinsic benefits and environmental considerations[88]. The low density and high specific strength of lightweight metal alloys, as well as other desirable features such as good corrosion resistance, dimensional stability, energy-saving capability, and sustainability, make them far more desirable. However, selecting the most capable LWEFM for a typical application based on a variety of parameters is challenging and presents a wonderful challenge for design engineers. On the other side, inappropriate material selection frequently results in premature product failure, resulting in decreased efficiency and performance.

Additional classifications for lightweight HEAs include refractory lightweight constituents e.g., Ti, V, and Nb, and extremely lightweight constituent e.g., Li, Mg, and Si. Lightweight, high entropy alloys (LWHEAs) have a density of less than 7 $g.cm^{-3}$ and are considered a subtype of high entropy alloys (HEAs). The work related to such research from across the world has had a significant impact on this discipline [89,90]. Juan et al. [91] produced $Al_{20}Be_{20}Fe_{10}Si_{15}Ti_{35}$ LWHEA using the casting process. The microstructure

had a density of 3.91 g cm^{-3} and a hardness of 911 HV, with the main phase being the predominant phase and two additional minor phases present. Youssef et al. [56] achieved a high hardness as well as low density (2.67 $g.cm^{-3}$) while making $Al_{20}Li_{20}Mg_{10}Sc_{20}Ti_{30}$ by cryo-milling, which established a single-phase FCC structure and then the microstructure was transformed into a Hexagonal Crystal. The $Al_{35}Cr_{14}Mg_6Ti_{35}V_{10}$ alloy with a hardness of 460 HV, obtained through mechanical alloying (MA) and compacted through the use of spark plasma sintering (SPS) is stronger than other traditional Al, Mg, and Ti-based alloys [92].

1.5 Thermal stability

One of the very exciting areas for the research community is the thermal stability of multicomponent alloys. This property of the alloys is the secret to qualifying them for use at higher temperatures. A favourable attribute of good mechanical properties is also the nanostructure nature of the alloy at a higher temperature [93,94]. HEAs are gaining more attention in this respect and emerging as a new physical metallurgy area [95]. Non-equilibrium manufacturing route-formed alloys, i.e., at room temperature, MA demonstrated the development of metastable phases. When subjected to heat treatment, their metastable phases can alter and shape new structures. The critical feature of thermal stability for the MAed HEAs is preserving the fine microstructure, slower grain growth, and regulated phase formation. Table 1.2 lists the phase stability of the different MA-processed HEAs. In AlFeCrCuTiZn HEA, Varalakshmi *et al.* [55] recorded high thermal stability by holding the BCC structure up to 800°Cfor one h. Christofidou *et al.* [96] reported phase stability in CrFeCoNi and $CrMn_xFeCoNi$ HEA at 500, 700 and 900 °C for 1000 h thermal exposure. In the solid solution of the FCC phase, however, the formation of $M_{23}C_6$ like carbide was observed, but when the concentration of Mn increased from 11.11 to 20 %, the alloy showed the formation of the sigma phase at 1000 h heat treatment.

The equilibrium structure was established on the other side by equilibrium processing routes, i.e., melting/casting, and most of them preserved their structures throughout thermal treatment. In the literature, developments of new secondary stages were also published.

1.6 Properties of HEAs

There is an enormous potential for manipulating the properties in the large ranges of composition design versatility of HEAs. The main effects of HEAs, which were discussed earlier, are due to many of their properties. This segment deals with the different properties of HEAs as follows:

1.6.1 Mechanical Behavior of HEAs

By controlling the composition and microstructure of the HEAs, major achievements have been developed for mechanical properties. Compared to the HEAs provided by the melting/casting route, the better mechanical properties of MAed HEAs are controlled by different strengthening mechanisms. HEAs demonstrate their strength in the melting/casting pathway, primarily derived from solid solution and precipitation strengthening. The commonly studied alloy method in the literature is AlxCoCrCuFeNi HEA [31,97]. The hardness variation from 133 HV to 655 HV by varying the concentration of Al (x= 0-3 at%) was shown in Figure 1.4 [98]. Al seems to be the enormously large atom amongst the component elements; the increased level of hardness is a result of the lattice deformation phenomenon. Furthermore, Al has a good affinity with other elements to form binary compounds, reinforcing the solid solution. The increase in Al concentration in the same line favors the development of BCC/B2 phases, which have been stronger than the FCC phase. With the transformation of phase from FCC to BCC, Figure 1.4 also showed the variance of crack length. For the BCC phase, which implies an increase in hardness, an increase in length was observed.

The crystal structure and phases present in the alloy influence the hardness of most of the Haskin Table 1.4, the typical range of hardness values for the various phases is given. At room temperature, the hardness of as-cast HEAs seem to be usually low, especially for the ones possessing the FCC phase[99]. On the other hand, those containing large amounts of Al and Ti are often more owing to the formation of strong secondary phases.

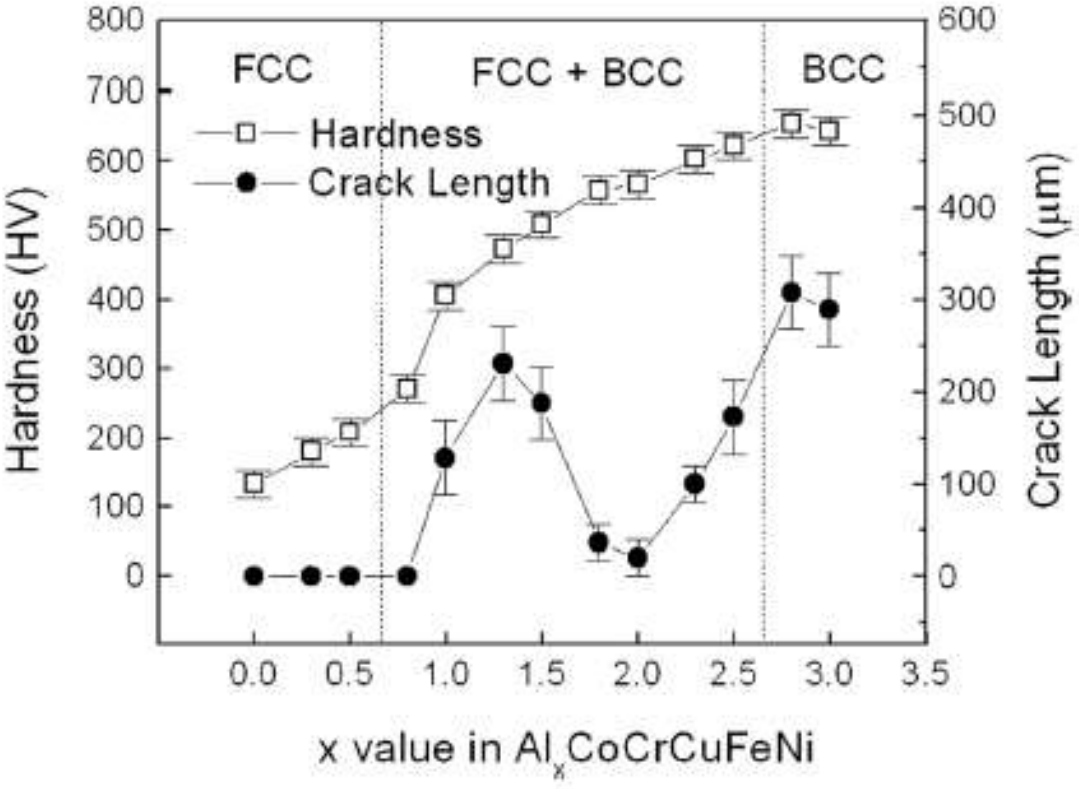

Figure 1.4: Variation of hardness (HV) and crack length around the indent by varying the Al concentration in theAlxCoCrCuNiFe alloy system [98].

The typical values of hardness of refractory high entropy alloys primarily comprised of the body-centered cubic (BCC) phase are quite high, for example 390 HV, 454 HV, 535 HV, 591 HV, is noticed for HfNbTaTiZrTi, MoNbTaW, MoNbTaVW, and $AlMo_{0.5}NbTa_{0.5}TiZr$, respectively [100]. Senkov et al. [76] discovered the minor effects of Al incorporation in the form of AlNbTaTiVZr and AlNbTaTiZr HEAs with

hardness values ranging from 30 to 81 HV, respectively. Similar effects were seen for compressive characteristics. Youssef et al. [56] demonstrated the development of solid solution with single face in mechanically alloyed $Al_{20}Li_{20}Mg_{20}Sc_{20}Ti_{20}$ HEA after 16 h. The milled powder exhibits a FCC phase with a hardness value of 5.8 GPa due to the nanostructured grains of 12 nm. Upon further annealing at 500 °C (773 K), this lightweight HEA structure transforms into an HCP structure. It retains its nanocrystalline structure, with 26 nm and 4.9 GPa of grain size and hardness, respectively [56]. Chen et al. [44] synthesized amorphous BeCoMgTi and BeCoMgTiZn HEAs by mechanically alloying elements with an HCP crystal structure. By employing the high energy ball milling (HEBM) of constituent powders and subsequently enhanced density using spark plasma sintering (SPS) technique, a multicomponent high entropy alloy (AlCuSiZnFe) has been synthesized.

It established the existence of a significant face-centered cubic (FCC) phase in (45 h) HEBMed powders, in addition to a small body-centered cubic (BCC) phase. The spark plasma technique has been employed for sintering of the samples at 600℃, 650℃ and 800 ℃. Microhardness of HEA rises with increasing SPS temperature in the range 690–974 HV [101].

Table1.4: Typical range of hardness values in HEAs based on their phase evolution[102].

Type	Phases	Hardness (HV)
BCC and derivatives	BCC, B2, Heusler	300-700
FCC and derivatives	FCC, $L1_2$, $L1_0$	100-300
Intermetallic phases	σ, Laves, η	650-1300
Valence compounds	Carbides, borides, silicides	1000-4000

The hardness of HEAs is reported to lie in a range between ~150 HV to 1200 HV [103,104] and this variation is reportedly dependent on the composition as well as on the methods being employed for synthesis [105]. The hardness of $Al_xCoCrCuFeNi$ rises with increasing Al content owing to the shift from a single-phase FCC configuration to a BCC+FCC configuration and eventually to a single-phase BCC configuration [9] . $Al_xCoCrFeNi$ alloys have a similar behavior under as-cast and homogenized circumstances [99]. Vickers hardness values for single-phase FCC alloys vary from 100 to 200 HV. However, the value of hardness exceeds 600 HV for single-phase BCC alloys. While for BCC+ FCC alloys, it has been noticed that the value of hardness rise with rising concentration of BCC elements. It has been established by the Transmission electron microscopy (TEM) that $Al_xCoCrCuFeNi$ alloys primarily identified as single-phase BCC structures by X-ray diffraction now have fine mixes of BCC and B2 phases [81,106]. Such phases are typically coherent which may attribute to the alloys remarkable hardness. Other alloys have likewise reported to improvement in the hardness as the ratio of BCC to B2 phases rises [107,108]. Increases in hardness are observed when the volume percentage of additional intermetallic phases in FCC or BCC microstructures is increased, like (D8b, tP30, Cr Fe model) or Laves (C14, hP12, $MgZn_2$ model or C15, cF24, model Cu_2Mg) [109–111].

Wu et al. [112] synthesized and studied temperature-dependent mechanical characteristics of equiatomic binary, ternary, quaternary, and non-equiatomic quinary alloys composed of Co, Cr, Fe, Mn, and Ni. As long as Cr is present, all binary, ternary, quaternary, and non-equiatomic quinary alloys exhibit comparable characteristics to the CoCrFeMnNi HEA. However, the absence of Cr decreases the strength in comparison to CoCrFeMnNi. The creation of the σ phase was found when the Cr content is above 26 at%, which boosts the strength. The elemental effect on the mechanical characteristics of HEAs

has been reviewed by Zongyang et al. [113]. It has been noted that Fe and Ni have demonstrated a detrimental effect on the strength of HEAs in most circumstances, while elements such as Mo, V, and Si have a positive effect on the strength. Zhou et al. [24] investigated the mechanical characteristics of $AlCoCrFeNiTi_x$ (x=0,0,5,1,1,5) HEA at room temperature. A $Ti_{0.5}$ alloy demonstrates high yield and fracture strength values with a small decrease in ductility, i.e., 2.26 GPa, 3.14 GPa, and 23.3 at %. Better properties are attributed to the solid solution reinforcement mechanism due to the Ti atoms. Having a larger atomic radius, Ti significantly distorted the lattice and increased the solid solution to strengthen the alloy. Heat treatment's influence on mechanical characteristics of AlCoCrFeNi HEA has been investigated by Munitz *et al.* [114]. The microhardness of the dendrite core (DC) regions has been reported to remain almost constant (4.5 GPa) in the 850-1100 ℃ range after heat treatment. After heat-treatment at 1200 ℃ in inter-dendritic areas, the hardness value increases (up to 5.4 GPa) and is due to the deposition of new nano-sized particles. The variation of compressive yield stress (σ_y) was observed in the same line with heat treatment temperatures. The yield stress (σ_y) of 1380 MPa, which increases up to 1690 MPa after heat treatment at 975℃ was shown by the as-cast alloy; this originated from the brittle σ phase's development in nature. The high strength (2988 MPa) and hardness (~ 704 HV) value of the $Co_{20}Ni_{20}Fe_{20}Al_{20}Ti_{20}$ HEA provided by MA and SPS was stated by Fu *et al* .[115]. Such higher mechanical property values are related to the B2 phase formation and the presence of Al_3Ti particles in the FCC matrix.

The wear behavior of $Al_{0.2}Co_{1.5}CrFeNi_{1.5}Ti$ HEA was studied by Chuang *et al.* [116]. The HEA wear resistance was compared to two traditional wear-resistant steels. The HEA has been found to have at least two times the higher wear resistance than conventional steels of comparable hardness. The wear resistance and friction coefficients of mechanically alloyed AlCrFeMnV and CuCrFeTiZn HEAs for the addition of Bi and Pb as

soft dispersoids have been investigated by Yadav *et al.* [117]. Wear resistance was boosted by ~20% in both cases, with a substantial decrease in friction coefficient. Alloys $Al_{0.4}Hf_{0.6}NbTaTiZr$ [33,76,100]. Therefore, the alloy system chosen, the composition proportion modification within the alloy system, and the alloy processing technique chosen all contribute significantly to the alloy hardness of HEAs. Due to its nanocrystalline structure, a low-density $Li_{20}Mg_{10}Al_{20}Sc_{20}Ti_{30}$HEA having a particle size of around 12nm on average of 606 HV [56]. Zhang et al. [104] also obtained a high hardness for the $(AlSiTiCrFeCoNiCuMo)B_{0.5}$ HEA, which has been produced through laser cladding and exhibits a martensite-like lath phase. Owing to the nucleation of the martensite phase during fast densification, this alloy possesses a high Vickers hardness of 1122 HV. The conventional BCC alloys and metals, the mechanical properties of compositionally complicated BCC solid formulations is extremely temperature dependent. With the exception of $Hf_{0.75}NbTa_{0.5}Ti_{1.5}Zr_{1.25}$, which was evaluated to cryogenic temperatures [118], the mechanical characteristics of BCC HEAs have indeed been investigated among room temperature and 1600 °C. Up to 600 °C, BCC solid solutions sustain yield strains greater than 500 MPa. Beyond 600 °C, mechanical characteristics deteriorate more or less dramatically, and at 800, 1000, and 1200 °C, a broad assortment of yielding stress were seen. Only MoNbTaW and MoNbTaVW sustain extraordinary strengths at elevated temperatures (> 1200 °C) (405 and 477 MPa at 1600 °C for MoNbTaW as well as for MoNbTaVW). When the specific strength of the BCC HEAs is considered, the gaps between them widen. $Al_{0.3}NbTa_{0.8}Ti_{1.4}V_{0.2}Zr_{1.3}$ is the most intriguing value at room temperature, 255 $MPa.g^{-1}.cm^3$ [112]. The highest specific yielding stress, around 130 and 180 $MPa.g^{-1}.cm^3$, are reported in the 400–800 °C region for annealed low-density AlCrMoTi and AlCrMoNbTi alloys [48,49]. At temperatures above 800 °C great majority of solid solutions lose their specific strength.

1.6.2 Physical Behavior

It has been established that HEAs have fascinating physical characteristics. Co, Fe, as well as Ni are all found in the majority of complex concentrated alloys (CCAs) that have been studied for their magnetic properties. CoFeNi indeed a ferromagnetic single-phase SS alloys characterized by an FCC crystal formation with a saturated magnetism (Ms) of 151 emu/g [119]. The FCC configuration in AlxCoFeNi is converted to FCC+ BCC/B2 or to FCC silicides in $CoFeNiSi_x$ by Al additives [119]. M_s drops to 102 emu/g as Al increases to one, and to 80.5 emu/g when Si increases from zero to 0.75. Magnetostriction does have a minor effect, yet it is required to protect substances against external magnetic fields.By integrating Al and Si in $(AlSi)_xCoFeNi$ (x= 0–0.8), the alloy's properties at x = 0.2 includes (Ms) coercively, electric resistivity, yield strength, as well as strain without breakage, which all contributes to the alloy's attractiveness as a softer magnetic material [119]. Addition of Al and Cr to un-homogenized $Al_xCoCrFeNi$ (x=0-2) alloys results in ferromagnetic properties between 5 and 50 K. Nonetheless, paramagnetic properties at 300 K as a result of shifting Ma et al. [120] discovered that the $AlCoCrFeNb_xNi$ (x=0, 0.1, 0.25, 0.5, and 0.75) HEA has ferromagnetic characteristics due to its permeability (χ) being in the range of 0.02-0.003, whereas the TiCoCrCuFeNi as well as TiCoCrCuFeNi alloys have superparamagnetic behavior owing to the formation of nanoparticles alloys. The annealing effect on the evolution of CoCrFeNiCuAl HEA's structure and properties was studied by Zhang *et al.* [121]. In both the as-cast and annealed stages, HEA exhibited superior soft magnetic characteristics. The saturation magnetization (Ms), retentivity ratio (Mr/Ms), and coactivity (Hc) of the as-cast and annealed alloys are determined to be 38.18 emu/g, 5.98 percentage, 45 Oe, and 16.08 emu/g, 3.01 percent, 15 Oe, and 15 Oe, correspondingly. Such quantities correspond to soft ferrite and can be utilized as delicate magnetic

substances. The coarsening of the granules and phase transformations occurred in a decrease in the as-annealed alloy's saturated magnetism (Ms).

1.7 Miedema's model: A Semi - empirical approach

The enthalpy of mixing (ΔH_{mix}) for HEAs may be calculated using Miedema's model. However, the semi-empirical model proposed by Miedema is applicable for computing the binary enthalpy of mixing. Therefore, for computing the ΔH_{mix} for HEA system, all the binary sub-systems are taken into consideration. The binary enthalpy of mixing was semi-empirically computed by thermodynamic data as suggested by Miedema et al. [122]. Binary values of enthalpy of mixing can be computed through the equation as follows.

$$\Delta H_{AB}^{mix} = 2P\, f(C^s) \frac{(C_A V_A^{\frac{2}{3}} + C_B V_B^{\frac{2}{3}})}{(n_{ws}^A)^{-\frac{1}{3}} + (n_{ws}^B)^{-\frac{1}{3}}} \times [-(\Delta\varphi^*)^2 + \frac{Q}{p}(n_{ws}^{1/3})^2 - \frac{R}{P}] \quad (1.10)$$

Where P, Q and R, are constants dependent on the type of metals forming the alloy

P = 14.1 (for transition- transition metal combination)

= 10.6 (for non-transition- non-transition metal combination)

= 12.3 (for transition- non-transition metal combination)

Q/P = 9.4 for all alloy systems

R = 0 for transition-transition metal alloys and non-transition-non-transition metal alloys

≠ 0 for alloys of transition metal with non-transition metal

f (c^s) = concentration function

= $c_A^s c_B^s$ for a regular solution or solid solution

$$c_A^S = \frac{c_A V_A^{2/3}}{(c_A V_A^{\frac{2}{3}} + c_B V_B^{\frac{2}{3}})} \quad (1.11)$$

$$c_B^S = \frac{c_B V_B^{\frac{2}{3}}}{\left(c_A V_A^{\frac{2}{3}} + c_B V_B^{\frac{2}{3}}\right)} \quad (1.12)$$

V_A, V_B= volume of A and B metal atoms

n_{WS}^A, n_{WS}^B= electron density parameter for metal atoms A and B, respectively

$\Delta\varphi^*$ = difference between the work functions of two elements considered

$n_{WS}^{-1/3}$, φ and $V^{2/3}$ values for different values can be obtained from ref [123]

For binary value enthalpy calculation of each pair present in our alloy system, it will be considered as $c_A^S = c_B^S$= ½; Regular solution model calculated net enthalpy of mixing opted from [39]

$$\Delta H_{mix} = \sum_{i=1, i\neq j}^{n} \Omega_{ij}\, C_i\, C_j \quad (1.13)$$

Where Ω_{ij}(=4ΔH_{AB}^{mix}) is a normal melt-interaction parameter among the i^{th} and j^{th} elements, and ΔH_{AB}^{mix} denotes the mixing enthalpy of the binary AB alloy. However, C_i,C_j represents the atomic concentration of the i^{th} andj^{th} components, respectively. If system is a five-component eqi-atomic alloy, we can consider $C_i = C_j$= 1/5.

1.8 CALPHAD: Phase Diagram Approach

The phase diagram are the graphical representation of the stable phases of the alloy system, as a function of pressure, temperature and concentration of component. In general the phase diagrams are computed at a constant pressure for binary and in case of ternary system it is expressed at constant pressure and temperature. However, for alloy systems

containing more elements the representation of phase diagram becomes difficult. A preliminary phase diagram can be predicted for the multicomponent system from the extrapolation of assessed constituent binary and ternary subsystems. These binary and ternary phase diagrams can be easily accessed from the commercially available databases, i.e. Thermo-Calc, PANDAT, and MTDATA etc. The CALPHAD method is comparatively more scientific as compared to the other empirical methods.

The mutual solubility in the Cantor alloy was understood with the help of CALPHAD technique by Zhang et al. [124]. The CALPHAD technique with dedicated databases have very good predictive ability to estimate the phases present, volume fraction of phases and transformation temperature of phases [125]. The phase stability of 130,000 equimolar alloys based on the 45 elements were investigated by Miracle et al. [13] and Senkov et al. [126,127] by using CALPHAD (calculating phase diagrams) using Thermo-Calc software. Similarly, Gao et al. [128] predicted the thermal stability of sixteen multicomponent alloys with single phase BCC structure using CALPHAD approach.

1.9 Prospective Applications of HEAs

It should be remembered that correct alloy selection and processing can result in the remarkable qualities described in the HEA literature for the specified applications. Scientific curiosity has convinced researchers of HEAs' ability to replace existing alloys in demanding and tight operating settings by giving greater performance and service life [26]. Several HEA implementations in the difficult field of the current state include the following:

a. For engine materials, reliability at elevated temperatures, resistance to oxidation, hot corrosion, and creep.

b. For tool materials, increased strength and durability at room and raised temperatures, wear resistance, and high impact strength with reduced friction.

c. Marine structures must be more resistant to corrosion and degradation in saltwater.

d. The criteria for light transportation substances increase the specific strength, longevity, fatigue life, creep resistance, and machinability.

e. Lower density fabrics, greater strength, and strong toughness, i.e., materials for the golf club head.

f. Constant thermal resistivity coefficient for electrical and magnetic materials and thermally stable magnetization.

g. A few high entropy composition are now a days explored for its applicability in the hydrogen storage.

1.10 Motivation

The most of HEAs so far studied are based on transition metals with or without addition of Al. Less number of them have incorporated lightweight non-transition metals like Mg and Si. In the present work focus was towards the synthesis of Mg, Si and Al containing low-density HEAs. For enhancing the strength of these LDHEAs, elements like Cr and Fe were considered to be added in an equiatomic ratio with Mg, Si and Al. Therefore, the first composition of MgAlSiCrFe LDHEA composition was designed. In the second LDHEA composition Ni was added to observe the effect of B2-type phase and its effect on phase stability and mechanical properties. Further, the third alloy system the Cu and Zn were added in MgAlSiCrFe-CuZn LDHEA for the exploring the possibility of formation of γ-type brass LDHEAs. Moreover, the possibility of solid solution formation, with the combination of the various elements having HCP, FCC, BCC and DC structures, were thought to be worth exploring.

The majority of them have been synthesized by the melting and casting process. MA, which is quite a more straightforward process to synthesize the HEAs, extends the solubility of constituent elements and overcomes the shortcoming of heterogeneity. Therefore, the present work is being carried out to research the process and microstructural evolution of HEAs with their stability.

1.11 Objectives

The primary objective of the present work is to understand phase evolution, thermal stability and indentation behavior of low-density high entropy alloys synthesized through mechanical alloying. Further, it will be interesting to study the consolidation of these LDHEA powders through SPS. The broad objectives are mentioned as follows:

I. Synthesis of nanocrystalline MgAlSiCrFe, MgAlSiCrFeNi and MgAlSiCrFeCuZn HEAs through mechanical alloying.
II. Alloying behavior and phase formation in LDHEAs during mechanical alloying.
III. Thermal stability of low-density HEAs powders.
IV. Fabrication of bulk MgAlSiCrFe, MgAlSiCrFeNi and MgAlSiCrFeCuZn LDHEA through spark plasma sintering.
V. Structural and microstructural investigation of LDHEAs powders and SPSed samples.
VI. Understanding the Indentation behavior of SPSed LDHEAs.